

Purified NPC1 Protein: II. Localization of Sterol Binding to a 240-Amino Acid Soluble Luminal Loop*

Rodney E. Infante[‡], Arun Radhakrishnan[‡], Lina Abi-Mosleh[‡],
Lisa N. Kinch[¶], Michael L. Wang[‡], Nick V. Grishin^{§¶},
Joseph L. Goldstein^{‡1}, and Michael S. Brown^{‡1}

From the Departments of [‡]Molecular Genetics and [§]Biochemistry and [¶]Howard Hughes Medical Institute, University of Texas Southwestern Medical Center at Dallas, Dallas, Texas 75390

Defects in Niemann-Pick, Type C-1 protein (NPC1) cause cholesterol, sphingolipids, phospholipids, and glycolipids to accumulate in lysosomes of liver, spleen, and brain. In cultured fibroblasts, NPC1 deficiency causes lysosomal retention of lipoprotein-derived cholesterol after uptake by receptor-mediated endocytosis. NPC1 contains 1278 amino acids that form 13 membrane-spanning helices and three large loops that project into the lumen of lysosomes. We earlier showed that NPC1 binds cholesterol and oxysterols. Here we localize the binding site to luminal loop-1, a 240-amino acid domain with 18 cysteines. When produced in cultured cells, luminal loop-1 was secreted as a soluble dimer. This loop bound [³H]cholesterol (K_d , 130 nM) and [³H]25-hydroxycholesterol (25-HC) (K_d , 10 nM) with one sterol binding site per dimer. Binding of both sterols was competed by oxysterols (24-, 25-, and 27-HC). Unlabeled cholesterol competed strongly for binding of [³H]cholesterol, but weakly for [³H]25-HC binding. Binding of [³H]cholesterol but not [³H]25-HC was inhibited by detergents. We also studied NPC2, a soluble protein whose deficiency causes a similar disease phenotype. NPC2 bound cholesterol, but not oxysterols. Epicholesterol and cholesteryl sulfate competed for [³H]cholesterol binding to NPC2, but not NPC1. Glutamine-79 in luminal loop-1 of NPC-1 is important for sterol binding; a Q79A mutation abolished binding of [³H]cholesterol and [³H]25-HC to full length NPC1. Nevertheless, the Q79A mutant restored cholesterol transport to NPC1-deficient CHO cells. Thus, the sterol binding site on luminal loop-1 is not essential for NPC1 function in fibroblasts, but it may function in other cells where NPC1 deficiency

produces more complicated lipid abnormalities.

INTRODUCTION

Through studies of humans with inborn errors of metabolism, scientists have uncovered many aspects of lipid biochemistry (1-3). One disorder that remains puzzling is the complex disease known as Niemann-Pick, Type C, which is caused by loss-of-function mutations in one of two different genes, NPC1 and NPC2² (4). The clinical spectrum in patients with this lipid storage disorder is wide. Most subjects manifest in childhood with a devastating syndrome that includes enlargement of liver and spleen, lung disease, and neurological degeneration manifested by ataxia, dysarthria, gaze palsies, and progressive dementia, usually resulting in death before age 20 (5). The liver and spleen accumulate unesterified cholesterol, sphingomyelin and a variety of phospholipids and glycosphingolipids. Brain tissue does not contain a gross excess of cholesterol or sphingomyelin, but there is a distinct elevation of glycosphingolipids (5). Recent studies of a mouse model of NPC1 disease indicate that neurons may accumulate excess cholesterol, but this accumulation is masked at a gross level by a decline in the amount of cholesterol in myelin (6).

Despite the wide variety of lipid abnormalities in organs of these patients, the functional abnormality in cultured fibroblasts is surprisingly simple (7). These cells exhibit a striking defect in the disposal of cholesterol that has entered the cell through receptor-mediated endocytosis initiated by binding to low density lipoprotein (LDL) receptors. After uptake in coated vesicles, ingested LDL is delivered to lysosomes where the cholesteryl esters, which constitute the bulk of its cholesterol, are hydrolyzed. The unesterified cholesterol exits

the lysosome and is transported to other organelles, including the endoplasmic reticulum (ER), where the cholesterol exerts two regulatory actions that maintain cholesterol homeostasis: 1) it blocks the ER exit and subsequent proteolytic activation of sterol regulatory element-binding proteins (SREBPs), which are transcription factors that increase cholesterol synthesis (8), and 2) it activates acyl CoA: cholesterol acyltransferase (ACAT), an enzyme that re-esterifies cholesterol for storage as cytoplasmic cholesteryl ester droplets (9, 10). In fibroblasts from NPC patients, LDL enters cells normally, and the cholesteryl esters are hydrolyzed in lysosomes, but the liberated cholesterol remains trapped as free cholesterol in lysosomes. As a result of this exit block, LDL-derived cholesterol fails to inhibit SREBP processing (11), and it fails to activate ACAT (7, 12). A similar defect occurs in fibroblasts from BALB/c *npc^{nh}* mice, a line of mice with an NPC phenotype (13), and in CT60 cells, a line of cultured Chinese hamster ovary (CHO) cells that were mutagenized and selected to have a defect in cholesterol release from lysosomes (14).

A major advance in understanding of NPC disease occurred when the first defective gene was identified by positional cloning (15). This gene encodes a 1278-amino acid integral membrane protein, now known as NPC1, that resides in late endosomes and lysosomes of cultured cells. Mutations in the murine version of NPC1 are responsible for the defect in BALB/c *npc^{nh}* mice, and the hamster version is defective in CT 60 cells.

Evidence indicates that NPC1 is a polytopic membrane protein with 13 membrane-spanning helices (16). The protein has a cleaved NH₂-terminal signal sequence that targets the protein for insertion into membranes, three large luminal loops, and a cytoplasmic COOH-terminal segment that includes a dileucine sequence that targets the protein to lysosomes (17). Helices 3-7 of mature NPC1 bear sequence homology to a sterol-sensing sequence that was found initially in Scap, a sterol-sensing protein of the ER (18). Similar sequences are found in the ER enzyme 3-hydroxy-3-methylglutaryl coenzyme A reductase (19) and in Patched, a receptor for Hedgehog, a protein morphogen that bears a covalently attached cholesterol moiety (18, 20). In Scap, this sequence was named the sterol-sensing domain (19), and it has been shown to bind cholesterol

(21, 22). Whether this sequence in the other proteins binds cholesterol or other sterols is unknown.

Approximately 5-10% of patients with NPC disease have a mutation in NPC2, a soluble protein that is partially sequestered in lysosomes, and partially secreted by cells (23). Cultured cells from subjects with NPC2 deficiency have the same defect in release of lysosomal cholesterol as do cells with an NPC1 mutation (24). NPC2 has been demonstrated to bind cholesterol (25-28), and a crystal structure of NPC2 with bound cholesterol sulfate has been solved (29). The similarity in phenotypes between NPC1 and NPC2 mutations strongly suggests that the two proteins function sequentially in a pathway that releases cholesterol from lysosomes, but the order of their actions has not been determined (30).

As described in the accompanying paper (11), we encountered NPC1 unexpectedly in a search for a membrane-bound protein that binds oxysterols such as 25-hydroxycholesterol (25-HC). When delivered to cells in ethanol, these oxysterols mimic the ER regulatory actions of cholesterol, i.e., they block SREBP cleavage and they activate ACAT (8, 11). However, oxysterols do not traverse lysosomes, and there is no evidence that they require the actions of NPC1 or NPC2 in order to reach the ER. We were therefore surprised to find that a purified membrane-bound, oxysterol-binding protein turned out to be NPC1. In further studies we showed that recombinant human NPC1 bound cholesterol as well as oxysterols, but cholesterol binding occurred only when the detergent concentration was reduced below micellar levels (11).

In the current studies we localize the sterol binding site in human NPC1 to luminal loop-1. Using recombinant DNA technology, we prepare luminal loop-1 as a soluble protein of 240 amino acids that is secreted by cells. Purified luminal loop-1 binds oxysterols and cholesterol with high affinity. We characterize this binding reaction and provide evidence that luminal loop-1 contains the majority, if not all, of the cholesterol binding activity of NPC1.

EXPERIMENTAL PROCEDURES

Materials – We obtained 1,2-diheptanoyl-*SN*-glycero-3-phosphocholine (DHPC) from Avanti Polar Lipids, Inc.; sodium

cholesteryl sulfate from Sigma; n-dodecyl- β -D-maltopyranoside (DDM) and CHAPS from Anatrace, Inc.; and bovine serum albumin (BSA) from Pierce (Cat. No. 23210). Radioisotopes, antibodies, sterols, chromatographic supplies, lipoproteins, lipoprotein-deficient serum (LPDS), and all other reagents (unless otherwise specified) were obtained from sources prepared as described in the accompanying paper (11).

Buffers – Buffer A contains 50 mM Tris-chloride at pH 7.4, 150 mM NaCl, and 0.004% (w/v) NP-40. Buffer B contains 50 mM Tris-chloride at pH 7.4, 100 mM KCl, and 1% NP-40. Buffer C contains 50 mM Tris-chloride at pH 7.4 and 150 mM NaCl. Buffer D contains 50 mM Tris-chloride at pH 7.4, 50 mM KCl, 10% (v/v) glycerol, 5 mM dithiothreitol, 1 mM sodium EDTA, and protease inhibitor mixture (1 μ g/ml pepstatin A, 2 μ g/ml aprotinin, 10 μ g/ml leupeptin, 200 μ M phenylmethylsulfonyl fluoride, and 25 μ g/ml of *N*-acetyl-leucinal-leucinal nonleucinal).

Plasmid Constructions – pCMV-NPC1-His₈-Flag encodes wild-type human NPC1 followed sequentially by eight histidines and a Flag tag under control of the cytomegalovirus (CMV) promoter. This plasmid was constructed as described in the accompanying paper (11). pCMV-NPC1(1-307;1254-1278)-His₈-Flag was constructed from pCMV-NPC1-His₈-Flag by site-directed mutagenesis (QuickChange II XL kit, Stratagene) using the 5'-oligonucleotide, 5'-CTCCGAGTACACTCCCATCGATAGC GTAAATAAAGCCAAAAGTTGTGCC-3' and the 3'-oligonucleotide,

5'-GGCACAACCTTTTGGCTTTATTTACGC TATCGATGGGAGTGTAGTCGGA-3'.

pCMV-NPC1(1-264)-His₈-Flag was constructed from pCMV-NPC1(1-307;1254-1278)-His₈-Flag by site-directed mutagenesis using the 5'-oligonucleotide, 5'-CCTGCTCCCTGGACGA TCCTTGGCCATCACCATCACCATCACCAT CACGACTAA-3' and the 3'-oligonucleotide, 5'-TTATAGTCGTGATGGTGATGGTGATG GTGATGGCCAAGGATCGTCCAGGGAGCA GG-3'. The coding region of each plasmid was sequenced to ensure integrity of the construct. Mutations in NPC1 were produced by site-directed mutagenesis of pCMV-NPC1(1-264)-His₈-Flag and pCMV-NPC1-His₈-Flag plasmids.

pCMV-NPC2-His₈ encodes wild-type human NPC2 followed sequentially by eight-histidines under control of the CMV promoter.

The plasmid was constructed from pCMV-NPC2 (Origene Technologies) by site-directed mutagenesis (QuickChange II XL kit, Stratagene). The coding region of pCMV-NPC2-His₈ was sequenced to ensure integrity of the construct.

pTK-HSV-BP-2 encodes wild-type *Herpes simplex* virus (HSV)-tagged human SREBP-2 under control of the thymidine kinase promoter (19).

Transfection of NPC1 and NPC2 Constructs in CHO Cells – CHO-K1 cells were grown and transfected in medium A (1:1 mixture of Ham's F12 medium and Dulbecco's modified Eagle's medium, 100 units/ml penicillin and 100 μ g/ml streptomycin sulfate) containing 5% (v/v) fetal calf serum (FCS) as described in the accompany paper (11). Each dish was transfected with one of the following plasmids: 5 μ g of pCMV-NPC1-His₈-Flag, 5 μ g of pCMV-NPC1(1-307;1254-1278)-His₈-Flag, 5 μ g of pCMV-NPC1(1-264)-His₈-Flag (wild-type or the indicated mutant versions), or 5 μ g of pCMV-NPC2-His₈. After 16 h, the transfected cells were used for purification of NPC1 proteins as described below.

Mutant CHO 4-4-19 cells, defective in NPC1 (31), were obtained from Laura Liscum (Tufts University School of Medicine, Boston, MA). The defective NPC1 in 4-4-19 cells results from an amino acid substitution (Gly660Arg).³ On day 0, 4-4-19 cells were set up in medium A containing 5% FCS at 2x10⁵ cells/60-mm dish. On day 2, each dish was transfected in OPTI-MEM (Gibco) with the indicated plasmid, using Lipofectamine 2000 according to the manufacturer's directions. After 5 h, the medium was switched to medium A containing 5% newborn calf LPDS. After 16 h, the cells were used for assays of ACAT and SREBP-2 processing.

Purification of Full Length NPC1 and Internally Deleted NPC1(1-307;1254-1278) from Transfected CHO Cells – Recombinant NPC1 proteins were overexpressed in CHO-K1 cells as described above and purified in buffer A or B by nickel and M2 anti-Flag agarose chromatography as previously described (11).

Purification of Secreted Forms of NPC1(25-264) and NPC2 from Medium of Transfected CHO Cells – Recombinant NPC1 and NPC2 proteins were overexpressed in CHO-K1 cells as described above. On day 3, the medium was switched to medium A containing

1% (v/v) Cellgro® ITS (Fisher Scientific). After 24 h, the medium was collected and fresh medium A containing 1% Cellgro® ITS was added. This was done for 3 consecutive days for each group of transfected cells. After each collection, the medium was subjected to centrifugation at 2,500 rpm for 5 min at 4°C and then filtered through an Express PLUS 0.22-µm filter apparatus (Millipore). Medium was stored at 4°C covered in aluminum foil. Gravity columns were each filled with a 20-ml slurry of Ni-NTA agarose beads, after which each column was pre-equilibrated with 4 column volumes of buffer C. Filtered medium (1 L per column) was then passed overnight at 4°C through each Ni-NTA agarose column ~1 ml/min. Each column was washed sequentially with 50 ml of buffer C containing 20 mM and 40 mM imidazole. Bound protein was eluted with 50 ml of buffer C containing 200 mM imidazole. The eluted fraction containing NPC1(25-264)-His₈-Flag or NPC2-His₈ was concentrated to 0.5 ml by using a spin concentrator with an Amicon Ultracel 30K or 10K Filter Device (Millipore), respectively. The concentrated material was then subjected to gel filtration chromatography on a 24-ml Superdex-200 column that was pre-equilibrated with buffer C. The fractions containing the peak A₂₈₀ activity and eluting between 12.5 and 15 ml (for NPC1(25-264)-His₈-Flag) or between 16 and 18 ml (for NPC2-His₈) were pooled, and their protein content was quantified by either the BCA kit (Pierce) or the Lowry method (32). The pooled proteins were subjected to SDS/PAGE followed by Coomassie staining to determine purity.

Ni-NTA Agarose Assay for ³H-Sterol Binding – For the standard assay of wild-type and mutant versions of NPC1 and NPC2, each reaction contained, in a final volume of 80 µl of buffer A, either [³H]25-HC (165-180 dpm/fmol) or [³H]cholesterol (132 dpm/fmol) delivered in ethanol (final ³H-sterol concentration, 10-400 nM), 1 µg of BSA as indicated, and varying amounts of NPC1 or NPC2 protein. After incubation for 4 h or 16 h at 4°C, the mixture was loaded onto a column packed with 0.3 ml of Ni-NTA Agarose beads (Qiagen) that had been pre-equilibrated with the appropriate assay buffer. Each column was washed for ~15 min with 5-6 ml of buffer B, except for the experiments described in Fig. 6. The protein-bound ³H-sterol was eluted with 250 mM imidazole in buffer B and quantified by

scintillation counting as previously described (Radhakrishnan et al., 2004). For competition experiments with unlabeled sterols, the standard assays were carried out in the presence of the indicated unlabeled sterol (0-3 µM) delivered in ethanol (final ethanol concentration, 1-4%). In each experiment, all tubes received the same amount of ethanol.

Glycosidase Treatments – Each reaction, in a final volume of 42 µl, was carried out according to the manufacturer's directions (New England BioLabs) for 16 h at 37°C with the indicated amount of purified protein in the presence or absence of 4000 units of Endo H or 5000 units of peptide N-glycosidase F (PNGase F).

SREBP-2 Processing in Cultured Cells – Mutant CHO 4-4-19 cells (defective in NPC1) were transfected as described above. On day 3, the medium was switched to medium A containing 5% newborn calf LPDS, 5 µM compactin, and 50 µM sodium mevalonate. On day 4, the cells received fresh medium A supplemented with 5% newborn calf LPDS and various concentrations of β-VLDL or 25-HC. After incubation at 37°C for 5 h, cells were treated with 25 µg/ml of *N*-acetyl-leucinal-leucinal-norleucinal for 1 h and then harvested. Duplicate dishes were pooled for preparation of nuclear extract and 100,000g membrane fractions, which were then analyzed by immunoblotting for SREBP-2 (described below).

Immunoblot Analysis – The procedure for immunoblot analysis and the concentrations of antibodies used are exactly as described in the accompanying paper (11) except for the use of one additional antibody. Epitope-tagged SREBP-2 was detected with 0.2 µg/ml of IgG-HSV-Tag™, a monoclonal antibody directed against the glycoprotein D epitope of *Herpes simplex* virus (Novagen, Inc).

ACAT Assay – The rate of incorporation of [¹⁴C]oleate into cholesterol [¹⁴C]oleate and [¹⁴C]triglycerides by intact cell monolayers was measured as previously described (33).

RESULTS

Localization of Oxysterol Binding Site in NPC1 – Fig. 1A shows a diagram of the postulated domain structure of human NPC1, a 1278-amino acid protein. The protein is believed to contain 13 putative transmembrane helices (16) that divide the protein into the

following structural domains: 1) a cleaved signal sequence (amino acids 1-24) (15); 2) luminal loop-1 (amino acids 25-264); 3) luminal loop-2 (amino acids 371-615); 4) a putative sterol-sensing domain (transmembrane helices 3-7, amino acids 616-791) (18, 20); 5) luminal loop-3 (amino acids 855-1098); and 6) a lysosomal targeting signal (LLNF) at the COOH-terminus (amino acids 1275-1278) (17).

To localize the region in NPC1 that binds 25-HC, we created plasmids encoding the first 307, 644, 809, or 1178 amino acids of the protein fused to a fragment comprising the COOH-terminal 24 amino acids, which contains the lysosomal targeting signal. The epitope-tagged proteins were purified as described for the full length protein in the accompanying paper (11). All of these internally deleted proteins bound [³H]25-HC with saturation kinetics that were similar to that of the full-length protein (data not shown). The smallest of these deleted proteins contain 332 NPC1-derived amino acids and is designated NPC1-His₈-Flag(1-307;1254-1278) (see bottom panel of Fig. 1A). Fig. 1B shows the migration of this internally deleted protein on SDS-PAGE as determined by immunoblotting (*lane 2*). Migration of the full-length protein is also shown (*lane 1*). Both proteins exhibited broad bands, presumably owing to extensive *N*-linked glycosylation. The internally deleted and full-length protein bound similar amounts of [³H]25-HC (Fig. 1C). Unlabeled 25-HC and 27-hydroxycholesterol (27-HC) competed effectively for the binding of [³H]25-HC. Unlabeled cholesterol and 19-hydroxycholesterol (19-HC) did not compete (Fig. 1D). The binding specificity of the internally deleted NPC1 with respect to oxysterols is thus similar to that of the full-length molecule (11).

Secretion and Purification of Luminal Loop-1 of NPC1 - In order to further define the oxysterol-binding site within the membrane-anchored, internally deleted NPC1(1-307;1254-1278), we made a further truncation from the COOH-terminus to remove the single transmembrane domain and the lysosomal targeting sequence. This protein, designated NPC1(25-264)-His₈-Flag, contains the signal sequence and luminal loop-1 as shown in Fig. 2A. Fig. 2B shows a comparison of the amino acid sequence of luminal loop-1 of human NPC1 with a consensus sequence that was derived

from the sequences of 12 vertebrate species, including 10 mammals. Of the 240 amino acids in this domain, 124 are invariant (Fig. 2B, *black boxes*). Eighteen of the invariant residues are cysteines (Fig. 2B, *yellow boxes*). The 12 vertebrate sequences are shown in Fig. 1SM.

When expressed in CHO cells by transfection, full-length NPC1-His₈-Flag and NPC1(1-307;1254-1278)-His₈-Flag were found exclusively in a 10⁵g pellet of cell membranes (Fig. 2C, *lanes 6 and 9*). In contrast, the vast bulk of NPC1(25-264)-His-Flag was secreted into the medium (*lane 10*). Note that the relative amount of the medium fraction applied to the gel was only one-fifth the amount of the cell supernatant and pellet fractions.

To purify luminal loop-1 from the medium of transfected CHO cells, the medium was subjected to Ni-chromatography followed by gel filtration chromatography in the absence of detergents (see "Experimental Procedures"). When stored at 4°C in buffer C (without detergent) at concentrations between 0.3-2.0 mg/ml, the protein retained full binding activity and continued to appear monodisperse on gel filtration. The calculated molecular mass for the protein component of the epitope-tagged luminal loop-1 is 28.7 kDa. However, the secreted protein migrated on SDS-PAGE as a diffuse band slightly above the 50-kDa marker (Fig. 3A, *lane 1*). Treatment of the secreted protein with the glycosidase PNGaseF under denaturing conditions caused the recombinant protein to migrate as a compact band close to the 30-kDa marker (data not shown). Thus, the diffuse migration is attributable to glycosylation of some or all of the 5 potential *N*-linked glycosylation sites in the loop (Fig. 2B). Upon gel filtration in the absence of detergents, this protein eluted as a single symmetrical peak corresponding to ~100 kDa (Fig. 3B). We believe that the 100-kDa species is a dimer. When the protein was analyzed by circular dichroism (Fig. 3C), it showed a spectrum characteristic of high α -helical content with minima at 207 and 222 nm (34, 35).

Binding Specificity of Luminal Loop-1 - To measure the binding of ³H-labeled sterols to purified NPC1(25-264)-His₈-Flag, we used an assay in which the protein was trapped on a nickel agarose column, and bound ³H-sterols were quantified by scintillation counting (11, 22). The binding reactions were conducted in a low concentration of NP-40 (0.004%), which is

slightly higher than the critical micellar concentration (CMC), which is 0.0015% (discussed below). Fig. 4A shows binding of [3 H]25-HC to NPC1(25-264)-His₈-Flag in the absence and presence of an excess of unlabeled 25-HC. Binding of [3 H]25-HC was saturable with an apparent K_d of 10 nM (average of 7 experiments). At saturation, we estimated that 1 molecule of [3 H]25-HC bound to ~1 dimer of NPC1(25-264)-His₈-Flag. Binding of [3 H]25-HC was inhibited by an excess of unlabeled 25-HC (Fig. 4A) and by similar concentrations of unlabeled 24-HC and 27-HC (see Fig. 7G).

We then tested the ability of luminal loop-1 to bind [3 H]cholesterol. As shown in Fig. 4B, this protein fragment bound [3 H]cholesterol with an apparent K_d of 130 nM (average of 7 experiments). At saturation, we estimated that 1 molecule of [3 H]cholesterol bound to ~1 dimer of NPC1(25-264)-His₈-Flag, a similar binding stoichiometry to that of [3 H]25-HC. The binding of [3 H]cholesterol was inhibited by an excess of unlabeled cholesterol. [3 H]Progesterone did not show saturable binding to NPC1(25-264)-His₈-Flag when tested at concentrations from 1-400 nM (data not shown).

In studies not shown, we found that the maximal binding of [3 H]cholesterol or [3 H]25-HC to NPC1(25-264)-His₈-Flag was similar over a pH range of 4-8. Moreover, binding of [3 H]25-HC or [3 H]cholesterol was not affected by the presence of EDTA up to 10 mM, but both binding activities were markedly decreased in the presence of 10 mM dithiothreitol, a reducing agent that would be expected to disrupt the multiple disulfide bonds that are postulated based on the cysteine-rich amino acid sequence of luminal loop-1.

To examine in more detail the binding of [3 H]25-HC and [3 H]cholesterol to luminal loop-1, we carried out competitive binding studies, as shown in Figs. 4C and 4D. When [3 H]25-HC was present at a concentration near its K_d (10 nM), unlabeled 25-HC competed with an IC₅₀ value of ~10 nM, whereas unlabeled cholesterol did not effectively compete except at concentrations of 3 μ M (Fig. 4C). When [3 H]cholesterol was present at a concentration near its K_d (130 nM), unlabeled cholesterol competed with an IC₅₀ of ~100 nM, whereas unlabeled 25-HC inhibited with an IC₅₀ ~5 nM (Fig. 4C). Thus, by two different assays (direct binding and competition), luminal loop-1 showed a 13- to 20-fold higher affinity for 25-

HC than cholesterol. Epicholesterol showed no ability to compete for binding of either [3 H]25-HC or [3 H]cholesterol (Figs. 4C and 4D). Moreover, 19-hydroxycholesterol, a cholesterol analogue with a hydroxyl group on the sterol nucleus, did not compete for the binding of [3 H]25-HC when tested at concentrations up to 3 μ M (data not shown).

In an accompanying paper (11), we determined that under the buffer and temperature conditions of our assays the CMC for NP-40 is 0.0015%, and we showed that full-length recombinant NPC1 bound [3 H]cholesterol most efficiently when the NP-40 detergent concentration was below its CMC. On the other hand, [3 H]25-HC bound to the protein at NP-40 concentrations up to 1%, which is greater than 600 times the CMC. Fig. 5A shows an experiment examining the effect of NP-40 on the binding of [3 H]cholesterol and [3 H]25-HC to luminal loop-1. Binding of [3 H]cholesterol was markedly reduced when the detergent concentration exceeded the CMC, whereas [3 H]25-HC binding was intact at detergent concentrations that were 1000-fold higher. To determine whether this differential sensitivity applied to other detergents, we measured the binding of [3 H]cholesterol and [3 H]25-HC in the presence of three other detergents at concentrations that were one-sixth of the CMC or 6-fold above the CMC (Fig. 5B). The CMC for each detergent was determined by a dye encapsulation method (36) under conditions that were identical to those of our binding assay, i.e., in buffer C at 4°C. Binding of [3 H]cholesterol was intact at the submicellar concentrations of all four detergents examined (NP-40, DDM, DHPC, and CHAPS). In each case, binding was markedly reduced at supramicellar detergent concentrations. This relationship held even though the CMC values for these four detergents varied over a range of nearly 100-fold (0.0015% for NP-40 to 0.2% for CHAPS). On the other hand, [3 H]25-HC was unaffected by the detergents except for CHAPS, which reduced binding at a concentration that was 6-fold above the CMC (Fig. 5B).

Mutational Analysis of Luminal Loop-1

— We subjected NPC1(25-264)-His₈-Flag to mutational analysis in order to pinpoint amino acids crucial for sterol binding. We focused on five residues (Q79, N103, Q117, F120, and Y157) that are conserved in 12 vertebrate NPC1 orthologs and that exhibit >75% identity among

homologs of NPC1 found in 76 eukaryotic species (data not shown). These residues were also chosen for their hydrogen-bonding potential (Q79, N103, and Q117) or for their ability to form ring-stacking interactions (F120 and Y157). Each of these residues was mutated to alanine (see Fig. 2C, *red boxes*). The two hydrophobic residues, F120 and Y157, were also mutated to methionine. In addition to these novel mutations, we reproduced six “clinical” mutations corresponding to substitutions in luminal loop-1 observed in patients with NPC1 disease (Q92R, T137M, P166S, N222S, D242H, and G248V; see Fig. 2C, *blue boxes*) (37). Plasmids encoding each mutant version of luminal loop-1 were expressed in CHO cells, and the recombinant proteins were purified from the medium in a similar manner to the wild-type version. All mutant proteins were secreted, and they all showed a normal behavior on gel filtration and SDS-PAGE. The data for the Q79A mutant is shown in Fig. 3. Of the 14 mutant proteins, only two of the novel mutants, Q79A and Q117A, showed an abnormality in sterol binding. The most striking abnormality was observed with the Q79A mutant, which showed no detectable binding of [3 H]25-HC (Fig. 6A) and a 40% decrease in maximal binding of [3 H]cholesterol (Fig. 6B). Similar results were obtained in 4 additional experiments involving 3 different preparations of purified luminal loop-1. Circular dichroism (CD) spectra of the Q79A protein was identical to that of the wild-type protein, indicating no major structural changes (Fig. 3C). Mutant Q117A also showed a 40% decrease in binding of [3 H]cholesterol (Fig. 6B), but only a slight decrease in [3 H]25-HC binding (Fig. 6A). Figs. 6C and 6D show the binding data for two of the clinical mutants, Q92R and T137M, both of which showed normal binding for both [3 H]25-HC and [3 H]cholesterol.

Sterol Binding Properties of Recombinant NPC2 and Luminal Domain-1 of NPC1 – About 5% of patients with Niemann-Pick, Type C disease harbor mutations in NPC2, a soluble 132-amino acid protein that is secreted into plasma and also resides within the cell, primarily in lysosomes (23). Previous studies have shown that NPC2 binds cholesterol with measured K_d values that range from 50 nM to 5 μ M in different laboratories (25–27). To compare the sterol binding properties of NPC1 and NPC2, we prepared a plasmid encoding

pCMV-NPC2-His₈, expressed it in CHO cells, and purified the secreted NPC2 using the same procedure as described for luminal loop-1 of NPC1. The calculated molecular mass of the secreted protein component of NPC2-His₈ is 15.7 kDa. However, purified NPC2-His₈ migrated on SDS-PAGE as 3 distinct bands (23, 21, and 18 kDa) as visualized by Coomassie staining (Fig. 7A). Previous studies showed that NPC2 contains three *N*-linked carbohydrate chains that contain mannose-6-phosphate (38). Treatment of purified NPC2-His₈ with the glycosidase endo H (which removes only high-mannose chains) reduced the molecular mass of band 2 from 21 to 19 kDa and band 3 from 18 to 16 kDa (Fig. 7A), whereas treatment with PNGase F (which removes all *N*-linked chains) reduced all 3 bands to the predicted protein molecular mass of 16 kDa (Fig. 7A). Gel filtration studies of the recombinant NPC2 showed that it eluted as a single symmetrical peak corresponding to ~20 kDa (data not shown).

When incubated with [3 H]cholesterol, NPC2-His₈ showed saturable binding with an apparent K_d of ~150 nM (Fig. 7C). The protein did not bind [3 H]25-HC (Fig. 7B). This all-or-none difference in binding of [3 H]cholesterol vs. [3 H]25-HC is in contrast to that of the luminal loop-1 of NPC1, which binds both [3 H]cholesterol (Fig. 7C) and [3 H]25-HC (Fig. 7B).

Competitive binding studies confirmed that NPC2-His₈ binds cholesterol but not 25-HC (Fig. 7D), two other iso-octyl oxysterols, 24-HC and 27-HC (Fig. 7F). The difference in sterol binding properties of NPC1 and NPC2 was further supported by the competition experiments in which epicholesterol and cholesteryl sulfate competed efficiently for [3 H]cholesterol binding to NPC2 (Figs. 7D and 7F), but not to NPC1(25–264) (Figs. 7E and 7G). Moreover, androstanol, a cholesterol analogue that lacks the iso-octyl side chain, did not compete for [3 H]cholesterol binding to either NPC1(25–264) or NPC2 when tested at concentrations up to 3 μ M (data not shown). These results are consistent with the recent studies of Liou, *et al.* (39), who assessed the sterol-binding specificity of NPC2 with a competition assay in which the labeled ligand was a fluorescent plant sterol (i.e., dehydroergosterol) and the competitor unlabeled sterols were each tested at a single

concentration. The most effective competitor was cholesteryl sulfate (100% inhibition), whereas the iso-octyl oxysterols showed either no competitive inhibition (25-HC) or a partial inhibition of ~35% (24-HC and 27-HC).

Sterol Binding Properties of Full-length Mutant NPC1(Q79A) – To determine whether the point mutation Q79A that disrupts 25-HC binding in luminal loop-1 of NPC1 also affects the binding properties of the full-length NPC1 molecule, we expressed and purified the Q79A mutant version of full-length NPC1-His₈-Flag in 0.004% NP-40 as described for the wild-type protein in the accompanying paper (11). As shown in the binding curves in Fig. 8A, [³H]25-HC did not bind to the Q79A mutant protein. The Q79A mutant protein also bound very little [³H]cholesterol as compared with the wild-type version (Fig. 8B).

Full-Length Mutant NPC1(Q79A) Restores NPC1 Function to CHO 4-4-19 Cells – The availability of a point mutation in the full-length NPC1 protein that abolishes its 25-HC binding activity provided the opportunity to determine whether oxysterol binding to wild-type NPC1 influences the transport of lipoprotein-derived cholesterol from endosomes/lysosomes to the ER. To test this hypothesis, we transfected wild-type and mutant versions of NPC1-His₈-Flag into CHO 4-4-19 cells, a mutant line of CHO cells with a deficiency of NPC1 function. In these cells, LDL and β -VLDL have a reduced ability to stimulate ACAT activity as measured by cholesteryl [¹⁴C]oleate formation in intact cells (31). On the other hand, 25-HC activates ACAT normally in these cells (31). Figure 9A shows an immunoblot of membrane extracts from CHO 4-4-19 cells that were transfected with cDNAs encoding wild-type and Q79A mutant versions of NPC1-His₈-Flag. As a result of this transient transfection, these cells expressed high levels of both versions of NPC1 as compared to the mock-transfected cells. When the transfected CHO 4-4-19 cells were incubated with β -VLDL, a cholesterol-rich lipoprotein that binds to LDL receptors with high affinity and delivers cholesterol to lysosomes (40), the cholesterol from β -VLDL reached the ER and markedly stimulated cholesteryl [¹⁴C]oleate formation in the cells expressing either the wild-type or the Q79A mutant version of NPC1, but not in the cells transfected with a control mock plasmid (Fig. 9B).

In wild-type cells, when cholesterol derived from β -VLDL reaches the ER, it prevents the exit of SREBP-2, thereby blocking its proteolytic processing (8). In mock-transfected CHO 4-4-19 cells, high concentrations of β -VLDL (30 μ g protein/ml) did not block SREBP-2 processing (Fig. 9C, lane 2). In contrast, when the CHO 4-4-19 cells were transfected with cDNAs encoding either wild-type NPC1 or its Q79A mutant version, β -VLDL blocked SREBP-2 processing at concentrations as low as 1 μ g protein/ml (Fig. 9D, lanes 4, 11). All three transfected CHO 4-4-19 cells (mock, NPC1 wild-type, and NPC1 Q79A mutant) responded to 25-HC (Fig. 9C, lane 3; Fig. 9D, lanes 8 and 15).

DISCUSSION

The current data reveal a saturable sterol binding site on luminal loop-1 of human NPC1. The importance of this 240-amino acid loop is revealed by its strong sequence conservation in all vertebrate orthologs of NPC1 and in related proteins from eukaryotes as remote as yeast. When isolated as a soluble, secreted protein, this loop appears to form a homodimer as indicated by gel filtration. At saturation, one molecule of cholesterol or 25-HC is bound to each dimer of luminal loop-1. Under the conditions of our *in vitro* assay, the affinity for 25-HC (K_d , 10 nM) was 13-fold higher than the affinity for [³H]cholesterol (K_d , 130 nM). Consistent with this difference, 25-HC was an effective competitor of cholesterol binding, whereas cholesterol was a poor competitor for 25-HC binding.

As we observed with full-length NPC1, binding of cholesterol, but not 25-HC to luminal loop-1 was sensitive to the concentration of detergent in the assay. Cholesterol binding was abolished by supramicellar concentrations of a variety of detergents, including uncharged detergents (NP-40 and DDM) and zwitterionic detergents (DHPC and CHAPS) (Fig. 5B). Of these detergents, CHAPS was the only one that partially reduced binding of 25-HC. We interpret this finding to indicate that cholesterol has a tendency to partition into micelles rather than to bind to luminal loop-1. If manifest within cells, this tendency might be important in regulating the ability of NPC1 to move cholesterol from one membrane compartment to another.

In this regard, it is interesting that NPC2 has been shown to transfer its bound cholesterol to phospholipid liposomes in a reaction that is accelerated by a phospholipid, lyso-bisphosphatidic acid (28). This observation was possible because Cheruku, et al. (28) observed that cholesterol binding quenches the tryptophan fluorescence of NPC2. In preliminary studies, we found that 25-HC binding to luminal loop-1 does not alter its tryptophan fluorescence. Other methods will have to be employed to test the ability of luminal loop-1 to transfer its bound sterols to membranes.

In the only previous study of cholesterol binding to NPC1, Ohgami, *et al.* (41) used a photoactivated analog of cholesterol (7,7-azocholesterol). They added a radiolabeled version of this compound to intact cells and observed crosslinking to NPC1. There was a marked reduction in crosslinking when the cells expressed a loss-of-function mutant of NPC1 with a substitution in the sterol-sensing domain (P692S). Whether this crosslinking was caused by direct binding to the sterol-sensing domain, or whether this domain played a permissive role, could not be determined from these studies. The sterol specificity of the crosslinking in terms of whether or not the cholesterol interaction was competed by oxysterols was also not determined.

In the current studies, we found evidence that luminal loop-1 is the sole oxysterol-binding site on NPC1, at least under the conditions of our *in vitro* assays. Thus, a point mutation in luminal loop-1 (Q79A) abolished binding of 25-HC to the soluble luminal loop-1 (Fig. 6A), and it also abolished binding to full-length recombinant NPC1 (Fig. 8A). The situation with regard to cholesterol binding is less clear. When produced in soluble luminal loop-1, the Q79A mutation reduced binding of [³H]cholesterol by about 40% (Fig. 6B), yet this mutation in full-length NPC1 abolished binding of [³H]cholesterol completely (Fig. 8B). This difference could be attributable to the sensitivity of the cholesterol binding reaction to the presence of detergents. It is possible that the Q79A mutation impairs cholesterol binding to the extent that it becomes more sensitive to the presence of even small amounts of detergent, and that the full-length protein has more detergent bound to it than does the soluble protein. The important question of whether luminal loop-1 is the sole cholesterol

binding site on NPC1 will not be resolved until *in vitro* assays can be performed with NPC1 in a more normal environment, either *in situ* in isolated membranes or after reconstitution in liposomes.

The difference in the specificity of sterol binding between NPC1 and NPC2 suggests major differences in the sterol binding pocket of the two proteins. Whereas luminal loop-1 of NPC1 and NPC2 both bound [³H]cholesterol with similar affinities, only NPC1 bound [³H]25-HC (Fig. 7B). Moreover, binding of [³H]cholesterol to NPC2 was inhibited by epicholesterol and cholesteryl sulfate, whereas binding to luminal loop-1 of NPC1 was not inhibited. The crystal structure of cholesteryl sulfate bound to NPC2 provides an explanation for the specificity of NPC2's binding reaction (29). The cholesterol moiety binds with its hydrophobic side chain deeply embedded in a hydrophobic pocket that molds itself to accommodate the side chain and thus would not be expected to tolerate the presence of a polar hydroxyl, a finding consistent with our experimental data showing that 24-HC, 25-HC, and 27-HC do not bind NPC2 (Fig. 7D). On the other hand, the 3-hydroxyl of cholesterol is fully exposed to solvent, and therefore the binding would not be disrupted by the α -orientation of this hydroxyl in epicholesterol. The sterol binding site on luminal loop-1 of NPC1 must be quite different. This site must be able to accommodate polar groups on the side chain since the addition of a 25-hydroxyl group increases the affinity of binding by 13-fold. The site must also recognize the 3-hydroxyl on the other end of the cholesterol molecule since binding strongly prefers the β -orientation. It should be possible to define the sterol binding site crystallographically since it is possible to produce large amounts of soluble, secreted luminal loop-1.

The major challenge for the future is to define the functional role, if any, of the sterol binding site on luminal loop-1 of NPC1. Sterol binding to this site does not seem to be important for the known function of NPC1 in fibroblasts. Thus, in NPC1-deficient cells 25-HC blocks SREBP cleavage (11), accelerates the degradation of 3-hydroxy-3-methylglutyl CoA reductase⁴, and activates ACAT in a normal manner (11, 12). Moreover, the Q79A mutant of NPC1, which does not bind sterols *in vitro*, nevertheless restored the ability of cholesterol-

carrying β -VLDL to activate ACAT and block SREBP-2 processing in mutant CHO cells that lack NPC1 function (Fig. 9). It should be noted that these latter studies all involved marked overexpression of the Q79A mutant using a strong CMV promoter and thus could be obscuring a sterol-dependent regulatory role for the luminal loop-1. Future studies will need to be done in stably transfected cells expressing wild type and mutant NPC1 under control of a weak promoter.

It is likely that the sterol binding site in luminal loop-1 is essential for some function of NPC1 that is required *in vivo*, but is not reflected in cultured fibroblasts. As noted in the Introduction, the lipid storage abnormalities and

the functional deficits in organs of NPC1-deficient humans and animals are complex and cannot be explained solely by the single cholesterol transport defect observed in fibroblasts. *In vivo* the affected cells are primarily hepatocytes, macrophages, neurons, and glia. Major accumulations of gangliosides and other phospholipids often outweigh the accumulations of unesterified cholesterol. It seems likely that in specific cell types NPC1 performs a regulatory role involving phospholipid and glycolipid metabolism and that the sterol binding site on luminal loop-1 may influence this role. This hypothesis is currently under exploration.

FOOTNOTES

*This work was supported by research grants from the National Institutes of Health (HL20948 and GM67165), Welch Foundation (I-1505), and the Perot Family Foundation. R.E.I. and M.L.W. were supported by the Medical Scientist Training Program Grant (5T32 GM08014). A.R. was the recipient of a postdoctoral fellowship from the Jane Coffin Childs Memorial Fund for Medical Research.

¹To whom correspondence should be addressed: Dept. of Molecular Genetics, University of Texas Southwestern Medical Center, 5323 Harry Hines Blvd., Dallas, TX 75390-9046. Tel: 214-648-2141; Fax: 214-648-8804; E-mail: joe.goldstein@utsouthwestern.edu or mike.brown@utsouthwestern.edu

²The abbreviations used are: ACAT, acyl-coenzyme A cholesterol acyltransferase; CMC, critical micellar concentration; CMV, cytomegalovirus; DDM, n-dodecyl- β -D-maltopyranoside; DHPC, 1,2-diheptanoyl-*SN*-glycero-3-phosphocholine; ER, endoplasmic reticulum; FCS, fetal calf serum; 25-HC, 25-hydroxycholesterol; LPDS, lipoprotein-deficient serum; NP-40, Nonidet P-40; NPC1, Niemann-Pick, Type C1 protein; NPC2, Niemann-Pick, Type C2 protein; SREBP, sterol regulatory element-binding protein; β -VLDL, β -migrating very low density lipoproteins.

³Personal communication from Laura Liscum (Tufts University School of Medicine, Boston, MA).

⁴R.E. Infante, L. Abi-Mosleh, M.S. Brown, and J.L. Goldstein, Unpublished observations.

ACKNOWLEDGMENTS

We thank Shomanike Head and Ijeoma Onwuneme for invaluable help with tissue culture; Debra Morgan for excellent technical support; our colleague Hyock Kwon for expert advice; and Laura Liscum for generously providing CHO cells deficient in NPC1.

References

1. Brady, R. O. (1978) *Annu. Rev. Biochem.* **47**, 687-713
2. Goldstein, J. L. and Brown, M. S. (2001) *Science* **292**, 1310-1312
3. Kolter, T. and Sandhoff, K. (2006) *Biochim. Biophys. Acta* **1758**, 2057-2079
4. Pentchev, P. G., Vanier, M. T., Suzuki, K., and Patterson, M. C. (1995) Niemann-Pick disease type C: A cellular cholesterol lipidosis. In Scriver, C. R., Beaudet, A. L., Sly, W. S., and Valle, D., editors. *The Metabolic and Molecular Basis of Inherited Disease*, McGraw-Hill Inc., New York
5. Vanier, M. T. and Millat, G. (2003) *Clin. Genet.* **64**, 269-281
6. Xie, C., Burns, D. K., Turley, S. D., and Dietschy, J. M. (2000) *J. Neuropathol. Exp. Neurol.* **59**, 1106-1117
7. Pentchev, P. G. (2004) *Biochim. Biophys. Acta* **1685**, 3-7
8. Goldstein, J. L., DeBose-Boyd, R. A., and Brown, M. S. (2006) *Cell* **124**, 35-46
9. Brown, M. S. and Goldstein, J. L. (1986) *Science* **232**, 34-47
10. Chang, C. C. Y., Huh, H. Y., Cadigan, K. M., and Chang, T. Y. (1993) *J. Biol. Chem.* **268**, 20747-20755
11. Infante, R. E., Abi-Mosleh, L., Radhakrishnan, A., Dale, J. D., Brown, M. S., and Goldstein, J. L. (2007) *J. Biol. Chem.* **Submitted for Publication**,
12. Liscum, L. and Faust, J. R. (1987) *J. Biol. Chem.* **262**, 17002-17008
13. Loftus, S. K., Morris, J. A., Carstea, E. D., Gu, J. Z., Cummings, C., Brown, A., Ellison, J., Ohno, K., Rosenfeld, M. A., Tagle, D. A., Pentchev, P. G., and Pavan, W. J. (1997) *Science* **277**, 232-235
14. Cadigan, K. M., Heider, J. G., and Chang, T.-Y. (1988) *J. Biol. Chem.* **263**, 274-282
15. Carstea, E. D., Morris, J. A., Coleman, K. G., Loftus, S. K., Zhang, D., Cummings, C., Gu, J., Rosenfeld, M. A., Pavan, W. J., Krizman, D. B., Nagle, J., Polymeropoulos, M. H., Sturley, S. L., Ioannou, Y. A., Higgins, M. E., Comly, M., Cooney, A., Brown, A., Kaneski, C. R., Blanchette-Mackie, J., Dwyer, N. K., Neufeld, E. B., Chang, T.-Y., Liscum, L., Strauss, J. F., III, Ohno, K., Zeigler, M., Carmi, R., Sokol, J., Markie, D., O'Neill, R. R., van Diggelen, O. P., Elleder, M., Patterson, M. C., Brady, R. O., Vanier, M. T., Pentchev, P. G., and Tagle, D. A. (1997) *Science* **277**, 228-231
16. Davies, J. P. and Ioannou, Y. A. (2000) *J. Biol. Chem.* **275**, 24367-24374
17. Watari, H., Blanchette-Mackie, E. J., Dwyer, N. K., Watari, M., Neufeld, E. B., Patel, S., Pentchev, P. G., and Strauss III, J. F. (1999) *J. Biol. Chem.* **274**, 21861-21866

18. Nohturfft, A., Brown, M. S., and Goldstein, J. L. (1998) *Proc. Natl. Acad. Sci. USA* **95**, 12848-12853
19. Hua, X., Sakai, J., Brown, M. S., and Goldstein, J. L. (1996) *J. Biol. Chem.* **271**, 10379-10384
20. Millard, E. E., Gale, S. E., Dudley, N., Zhang, J., Schaffer, J. E., and Ory, D. S. (2005) *J. Biol. Chem.* **280**, 28581-28590
21. Radhakrishnan, A., Sun, L.-P., Kwon, H. J., Brown, M. S., and Goldstein, J. L. (2004) *Mol. Cell* **15**, 259-268
22. Radhakrishnan, A., Ikeda, Y., Kwon, H. J., Brown, M. S., and Goldstein, J. L. (2007) *Proc. Natl. Acad. Sci. USA* **104**, 6511-6518
23. Naureckiene, S., Sleat, D. E., Lackland, H., Fensom, A., Vanier, M. T., Wattiaux, R., Jadot, M., and Lobel, P. (2000) *Science* **290**, 2298-2301
24. Frolov, A., Zielinski, S. E., Crowley, J. R., Dudley-Rucker, N., Schaffer, J. E., and Ory, D. S. (2003) *J. Biol. Chem.* **278**, 25517-25525
25. Okamura, N., Kiuchi, S., Tamba, M., Kashima, T., Hiramoto, S., Baba, T., Dacheux, F., Dacheux, J.-L., Sugita, Y., and Jin, Y.-Z. (1999) *Biochim. Biophys. Acta* **1438**, 377-387
26. Ko, D. C., Binkley, J., Sidow, A., and Scott, M. P. (2003) *Proc. Natl. Acad. Sci. USA* **100**, 2518-2525
27. Friedland, N., Liou, H.-L., Lobel, P., and Stock, A. M. (2003) *Proc. Natl. Acad. Sci. USA* **100**, 2512-2517
28. Cheruku, S. R., Xu, Z., Dutia, R., Lobel, P., and Storch, J. (2006) *J. Biol. Chem.* **281**, 31594-31604
29. Xu, S., Benoff, B., Liou, H.-L., Lobel, P., and Stock, A. M. (2007) *J. Biol. Chem.* **282**, 23525-23531
30. Sleat, D. E., Wiseman, J. A., El-Banna, M., Price, S. M., Verot, L., Shen, M. M., Tint, G. S., Vanier, M. T., Walkley, S. U., and Lobel, P. (2004) *Proc. Natl. Acad. Sci. USA* **101**, 5886-5891
31. Dahl, N. K., Reed, K. L., Daunais, M. S., Faust, J. R., and Liscum, L. (1992) *J. Biol. Chem.* **267**, 4889-4896
32. Lowry, O. H., Rosebrough, N. J., Farr, A. L., and Randall, R. J. (1951) *J. Biol. Chem.* **193**, 265-275
33. Goldstein, J. L., Basu, S. K., and Brown, M. S. (1983) *Meth. Enzymol.* **98**, 241-260
34. Tinoco, I. and Woody, R. W. (1963) *J. Chem. Phys.* **38**, 1117-1125
35. Chen, Y.-H., Yang, J. T., and Chau, K. H. (1974) *Biochem.* **13**, 3350-3359

36. Fisher, L. E., Engelman, D. M., and Sturgis, J. N. (2003) *Biophys. J.* **85**, 3097-3105
37. Scott, C. and Ioannou, Y. A. (2004) *Biochim. Biophys. Acta* **1685**, 8-13
38. Chikh, K., Vey, S., Simonot, C., Vanier, M. T., and Millat, G. (2004) *Mol. Gen. Metabol.* **83**, 220-230
39. Liou, H.-L., Dixit, S. S., Xu, S., Tint, G. S., Stock, A. M., and Lobel, P. (2006) *J. Biol. Chem.* **281**, 36710-36723
40. van Driel, I. R., Goldstein, J. L., Sudhof, T. C., and Brown, M. S. (1987) *J. Biol. Chem.* **262**, 17443-17449
41. Ohgami, N., Ko, D. C., Thomas, M., Scott, M. P., Chang, C. C. Y., and Chang, T.-Y. (2004) *Proc. Natl. Acad. Sci. USA* **101**, 12473-12478
42. Adams, C. M., Reitz, J., DeBrabander, J. K., Feramisco, J. D., Brown, M. S., and Goldstein, J. L. (2004) *J. Biol. Chem.* **279**, 52772-52780

FIGURE LEGENDS

Fig. 1. Identification of oxysterol-binding site in recombinant human NPC1. *A*, predicted topology of full-length (*top panel*) and internally deleted NPC1 (*bottom panel*). The domain structure of NPC1 is discussed in Results. *B*, immunoblot analysis of equimolar amounts of full-length (*lane 1*) and NPC1-His₈-Flag (1-307;1254-1278) (*lane 2*). *C*, saturation curves for [³H]25-HC binding to full-length and NPC1-His₈-Flag (1-307;1254-1278). Binding assays were carried out as described under “Experimental Procedures” except that [³H]25-HC and unlabeled 25-HC were solubilized in 1% NP-40 as described in the accompanying paper (11). Each reaction, in a final volume of 120 μl of buffer B (1% NP-40), contained 200 ng of purified human full-length NPC1 (*circles*) or 60 ng of purified internally deleted NPC1 (*triangles*) and 0-300 nM [³H]25-HC (solubilized in 1% NP-40) in the absence (*closed symbols*) or presence (*open symbols*) of 8 μM unlabeled 25-HC (solubilized in 1% NP-40). After incubation for 3 h at 4°C, bound [³H]25-HC was measured using the Ni-NTA agarose binding assay as described under “Experimental Procedures.” Each data point represents total binding without subtraction of blank values. *D*, competitive binding of [³H]25-HC to internally deleted NPC1. Each assay tube, in a total volume of 120 μl of buffer B (1% NP-40), contained 300 ng of NPC1-His₈-Flag (1-307;1254-1278), 100 nM [³H]25-HC (solubilized in 1% NP-40), and varying concentrations of the indicated unlabeled sterol (solubilized in 1% NP-40). After incubation for 3 h at 4°C, bound [³H]25-HC was measured as described in *C*. Each data point represents the amount of [³H]25-HC bound relative to that in the control tube, which contained no unlabeled sterol. The “100% of control” value was 247 fmol/tube. 19-HC, 19-hydroxycholesterol; 27-HC, 27-hydroxycholesterol.

Fig. 2. Secretion of luminal loop-1 of NPC1. *A*, diagrammatic illustration of NPC1(25-264)His₈-Flag, showing the cleaved signal sequence (amino acids 1-24) and the secreted soluble domain (amino acids 25-264). *B*, comparison of the amino acid sequence of human NPC1(22-264) with the consensus sequence of luminal loop-1 from 12 vertebrate species. *Black boxes* denote residues invariant in all 12 vertebrate proteins. *White boxes* denote residues conserved in at least 50% of the aligned vertebrate sequences and are identical to the human sequence. *Yellow boxes* denote cysteine residues. *Red triangles* denote “novel mutations,” i.e., alanine or methionine substitutions, created by site-directed mutagenesis. *Blue triangles* denote “clinical mutations,” i.e., substitutions corresponding to naturally occurring mutations in patients with NPC1 disease. *Asterisks (*)* denote location of 5 potential N-linked glycosylation sites in the human sequence. *C*, immunoblot analysis of secreted NPC1(25-264). On day 0, CHO-K1 cells were set up and transfected with 5 μg pcDNA3.1 (mock), 5 μg pCMV-NPC1-His₈-Flag,

5 μ g pCMV-NPC1(1-307;1254-1278)-His₈-Flag, or 5 μ g pCMV-NPC1(1-264)-His₈-FLAG as described in “Experimental Procedures.” After incubation for 48 h at 37°C, the medium was collected, and the cells were washed and homogenized through a 1-ml syringe with a 22-gauge needle in 0.6 ml of buffer D. The homogenate was centrifuged at 10⁵g, after which the supernatant was collected and the pellet was solubilized in 10 mM Tris-chloride at pH 7.4, 100 mM NaCl, and 1% SDS and shaken at 37°C overnight. Fractions of medium (m), supernatant (s), and 10⁵g pellet (p) were applied to the gel in a 1:5:5 ratio, respectively, and then subjected to 8% SDS/PAGE and immunoblot analysis using monoclonal anti-Flag antibody. The filter was exposed to X-ray film for 30 s.

Fig. 3. Characterization of secreted NPC1(25-264). *A*, Coomassie staining. Recombinant NPC1(25-264) proteins were purified in two steps as described in “Experimental Procedures.” Aliquots (5 μ g) of wild-type and the Q79A mutant version of NPC1(25-264)-His₈-Flag were subjected to 8% SDS/PAGE, and the proteins were visualized with Coomassie brilliant blue R-250 stain (Bio-Rad). Molecular masses of protein standards are indicated. *B*, gel filtration chromatography of purified proteins. Buffer C (0.5 ml) containing 60 μ g of either wild-type or Q79A mutant version of NPC1(25-264)-His₈-Flag was loaded onto a 10/300 Superdex 200 column and chromatographed at a flow rate of 0.5 ml/min. Absorbance at 280 nm was monitored continuously to identify the indicated NPC1 protein. Standard molecular mass markers (thyroglobulin, 670 kDa; γ -globulin, 158; ovalbumin, 44; myoglobin, 17; and vitamin B12, 1.35) were chromatographed on the same column (arrows). The apparent molecular mass of NPC1(25-264)-His₈-Flag is ~100 kDa. *C*, circular dichroism of 200 μ g of wild-type or Q79A mutant version of NPC1(25-264)-His₈-Flag in buffer C was measured on an Aviv 62DS spectrometer using a 2-mm path length cuvette. The data shown represent the averaged values from 9 spectra.

Fig. 4. [³H]25-HC and [³H]cholesterol binding activities of purified NPC1(25-264). *A* and *B*, saturation curves for NPC1(25-264) binding of [³H]25-HC and [³H]cholesterol. Each reaction, in a final volume of 80 μ l of buffer A (0.004% NP-40), contained 100 ng of purified human NPC1(25-264)-His₈-Flag, 1 μ g of BSA, and 10-300 nM of either [³H]25-HC (*A*) or [³H]cholesterol (*B*) both delivered in ethanol, in the absence (black) or presence of 3 μ M unlabeled 25-HC (blue) or cholesterol (red) as indicated. After incubation for 4 h at 4°C, bound [³H]25-HC (*A*) or [³H]cholesterol (*B*) was measured using the Ni-NTA agarose binding assay as described under “Experimental Procedures.” Each data point is the average of duplicate assays and represents total binding without subtraction of blank values. *C* and *D*, competitive binding of [³H]25-HC (*C*) and [³H]cholesterol (*D*) to NPC1(25-264). Each assay tube, in a total volume of 80 μ l of buffer A (0.004% NP-40), contained 100 ng NPC1(25-264)-His₈-Flag, 1 μ g of BSA, either 10 nM [³H]25-HC (*C*) or 130 nM [³H]cholesterol (*D*), and varying concentrations of the indicated unlabeled sterol. After incubation at 4°C for 16 h, bound [³H]25-HC (*C*) or [³H]cholesterol (*D*) was measured using the Ni-NTA agarose binding assay. Each data point is the average of duplicate assays and represents the amount of ³H-sterol bound relative to that in the control tube, which contained no unlabeled sterol. The “100% of control” values were 340 fmol/tube (*C*) and 580 fmol/tube (*D*). Blank values of 3 fmol/tube (*C*) and 68 fmol/tube (*D*) were subtracted from these values.

Fig. 5. Detergent effects on ³H-sterol binding activity of NPC1(25-264). *A* and *B*, each assay tube, in a total volume of 80 μ l of buffer C supplemented with the indicated detergent (see below), contained 100 ng NPC1(25-264)-His₈-Flag, 1 μ g of BSA, and 200 nM [³H]25-HC (\blacktriangle) or [³H]cholesterol (\bullet). After incubation at 4°C for 4 h, bound [³H]25-HC or [³H]cholesterol was measured using the Ni-NTA agarose binding assay. Each data point is the average of duplicate values and represents the amount of ³H-sterol bound relative to that in the control tube, which contained no detergent. *A*, buffer C was supplemented with the indicated concentration of NP-40. The “100% of control” values were 391 and 236 fmol/tube for [³H]cholesterol and [³H]25-HC, respectively. *B*, buffer C was supplemented with the indicated detergent concentrations relative to its CMC. The CMC’s, determined in buffer C at 4°C, were as follows: NP-40, 0.0015%; DDM, 0.002%; DHPC, 0.06%; and CHAPS, 0.2%. The “100% of control” values for [³H]cholesterol and [³H]25-HC were 237 fmol/tube and 511 fmol/tube, respectively.

Fig. 6. [^3H]25-HC and [^3H]cholesterol binding to versions of NPC1 corresponding to novel mutations in conserved residues and clinical mutations in patients with NPC1. *A-D*, saturation curves for ^3H -sterol binding to wild-type and mutant NPC1 proteins. Each reaction, in a final volume of 80 μl of buffer A (0.004% NP-40), contained 100 ng of purified wild-type or the indicated mutant version of NPC1(25-264)-His₈-Flag, 1 μg of BSA, and 10-300 nM of either [^3H]25-HC (*A* and *C*) or [^3H]cholesterol (*B* and *D*), both delivered in ethanol. After incubation for 4 h at 4°C, bound [^3H]25-HC (*A*) or [^3H]cholesterol (*B*) was measured using the Ni-NTA agarose binding assay as described under “Experimental Procedures.” Each data point is the average of duplicate assays and represents total binding without subtraction of blank values.

Fig. 7. Comparison of the ^3H -sterol binding activities of purified NPC1(25-264) and purified NPC2. *A*, Coomassie staining of purified NPC2 before and after glycosidase treatment. Purified NPC2-His₈ (7.6 μg) was treated with or without Endo H or PNGase F as described under “Experimental Procedures” and then subjected to 15% SDS-PAGE, and the proteins were visualized with Coomassie brilliant blue R-250. Molecular masses of protein standards are indicated. Asterisks (*) denote the migration of Endo H (*lane 2*) and PNGase F (*lane 3*). Bands 1-3 denote different glycosylated forms of purified NPC2-His₈. *B* and *C*, saturation curves for binding of ^3H -sterols to NPC1(25-264) and NPC2. Each reaction, in a final volume of 80 μl of buffer A (0.004% NP-40), contained either 290 ng of purified human NPC2 (\blacktriangle) or 200 ng of purified human NPC1(25-264)-His₈-Flag (\bullet), 1 μg of BSA, and 0-400 nM of [^3H]25-HC (*B*) or [^3H]cholesterol (*C*), both delivered in ethanol. After incubation at 4°C for 16 h, bound ^3H -sterols were measured using the Ni-NTA agarose binding assay as described under “Experimental Procedures” except that the column washes were done with buffer A. Each data point is the average of duplicate values and represents total binding without subtraction of blank values. *D-G*, competitive binding of [^3H]cholesterol to NPC2 and NPC1(25-264). Each assay tube, in a total volume of 80 μl of buffer A (0.004% NP-40), contained either 200 ng of NPC2-His₈ (*D* and *F*) or 150 ng of NPC1(25-264)-His₈-Flag (*E* and *G*), 1 μg of BSA, 200 nM [^3H]cholesterol, and varying concentrations of the indicated unlabeled sterol. After incubation for 4 h at 4°C, bound [^3H]cholesterol was measured as described above. Each data point is the average of duplicate assays and represents the amount of [^3H]cholesterol bound relative to that in the control tube, which contained no unlabeled sterol. The “100% of control” values in fmol/tube were 1608 (*D*), 685 (*E*), 1555 (*F*), and 735 (*G*). Blank values of 25 to 71 fmol/tube were subtracted.

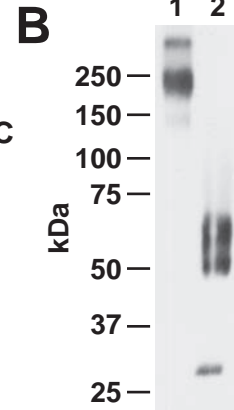
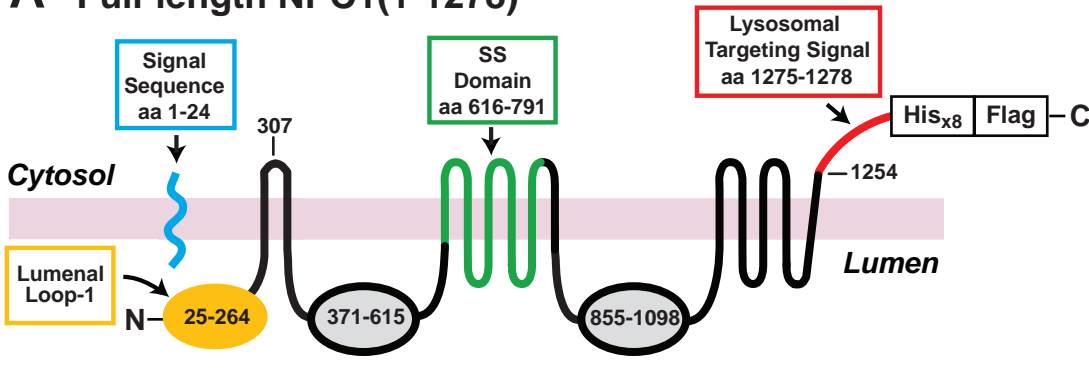
Fig. 8. [^3H]25-HC and [^3H]cholesterol binding activities of wild-type and mutant Q79A versions of full-length NPC1. Each reaction, in a final volume of 80 μl of buffer C (no NP-40), contained ~50 ng of human NPC1-His₈-Flag (\bullet) or NPC1-His₈-Flag(Q79A) (\blacktriangle) purified in 0.004% NP-40, 1 μg of BSA, and 10-300 nM of either [^3H]25-HC (*A*) or [^3H]cholesterol (*B*), both delivered in ethanol. The final combination of NP-40 was ~0.0008%. After incubation for 16 h at 4°C, bound [^3H]25-HC (*A*) or [^3H]cholesterol (*B*) was measured using the Ni-NTA agarose binding assay as described under “Experimental Procedures.” Each data point is the average of duplicate assays and represents total binding without subtraction of blank values.

Fig. 9 Regulatory actions of transfected wild-type and mutant Q79A versions of full-length NPC1 in mutant CHO 4-4-19 cells defective in NPC1. On day 0, mutant CHO 4-4-19 cells were set up in medium A containing 5% FCS as described in “Experimental Procedures.” *A*, immunoblot analysis of NPC1 proteins. On day 2, the cells were transfected with 2 μg pcDNA3.1 (mock, M) or 2 μg of wild-type or mutant Q79A version of pCMV-NPC1-His₈-Flag as described in “Experimental Procedures.” On day 3, the cells were harvested, and whole cell extracts were prepared (42) and processed for immunoblot analysis of the indicated proteins. *B*, cholesterol esterification assay in mutant CHO cells. On day 2, the cells were transfected as described in *A*. On day 3, the medium was switched to medium A containing 5% newborn calf LPDS, 5 μM compactin, and 50 μM sodium mevalonate. On day 4, the medium was switched to medium A supplemented with 5% newborn calf LPDS and the indicated concentration of β -VLDL. After incubation for 5 h at 37°C, each monolayer was pulse-labeled for 2 h with 0.2 mM sodium [^{14}C]oleate (6446 dpm/pmol). The cells were then harvested for measurement of their content of cholesteryl [^{14}C]oleate and [^{14}C]triglycerides as described under “Experimental Procedures.” Each value

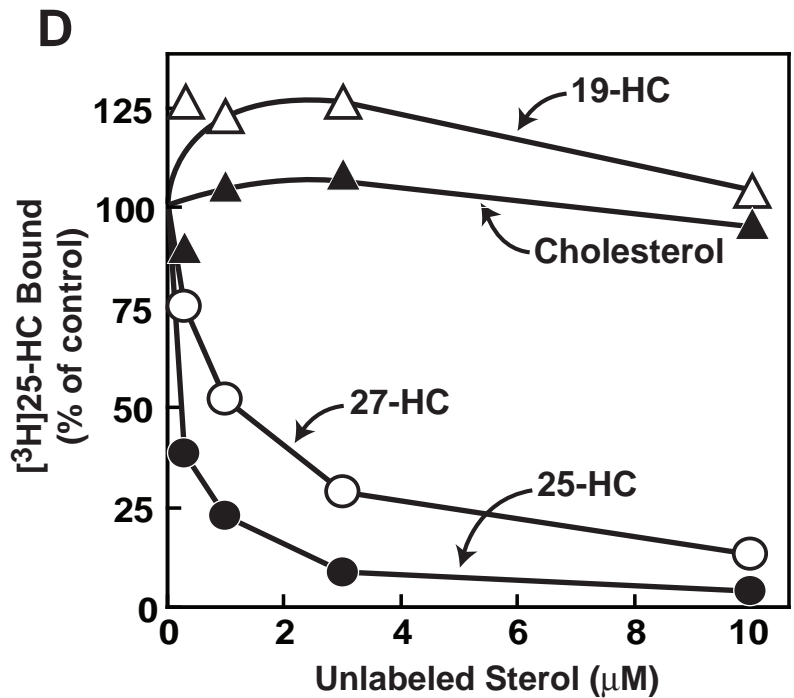
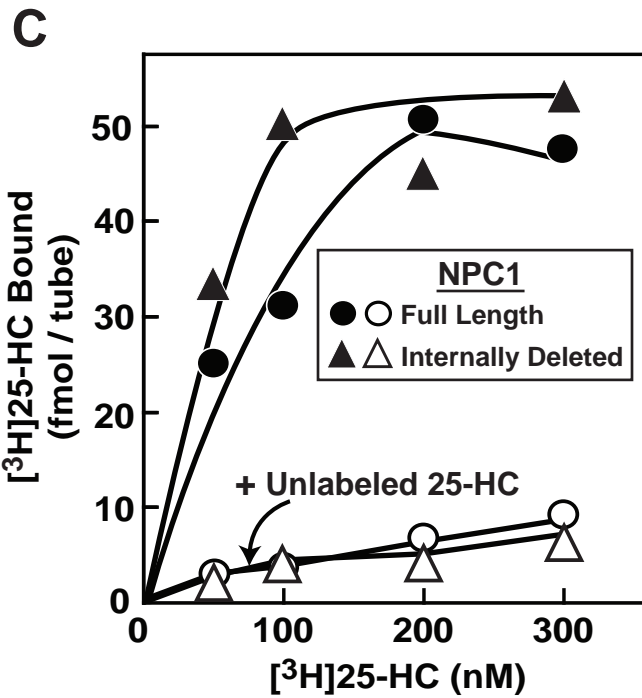
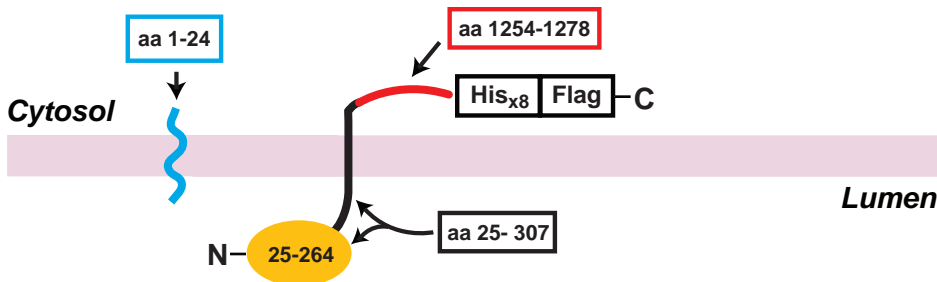
is the average of duplicate incubations. The cellular content of [^{14}C]triglycerides (data not shown in Fig.) for mock, NPC1 wild-type, or NPC1(Q79A) transfected cells incubated with 10 μg protein/ml of β -VLDL were 209, 184, and 194 nmol/h per mg, respectively. *C*, immunoblot analysis of SREBP-2 in mutant CHO cells overexpressing SREBP-2. On day 2, the cells were transfected with 3 μg of pTK-HSV-BP2. *D*, immunoblot analysis of SREBP-2 cleavage in mutant CHO cells overexpressing full-length NPC1 (wild-type or Q79A). On day 2, the cells were either mock transfected with pcDNA3.1 (M) or co-transfected with 3 μg pTK-HSV-BP-2 together with 2 μg of either wild-type or mutant Q79A version of pCMV-NPC1-Flag. *C* and *D*, on day 3, the medium was switched to medium A supplemented with 5% newborn calf LPDS, 5 μM compactin, and 50 μM sodium mevalonate. On day 4, the medium was switched to medium A supplemented with 5% newborn calf LPDS with the indicated concentration of β -VLDL or 1 $\mu\text{g}/\text{ml}$ of 25-HC. After incubation for 6 h, the cells were harvested and processed for immunoblot analysis of the indicated proteins. *A* and *C*, all filters were exposed on X-ray film for 5-10 s except for the nuclear SREBP-2 filter, which was exposed for 20 s.

Fig. 1

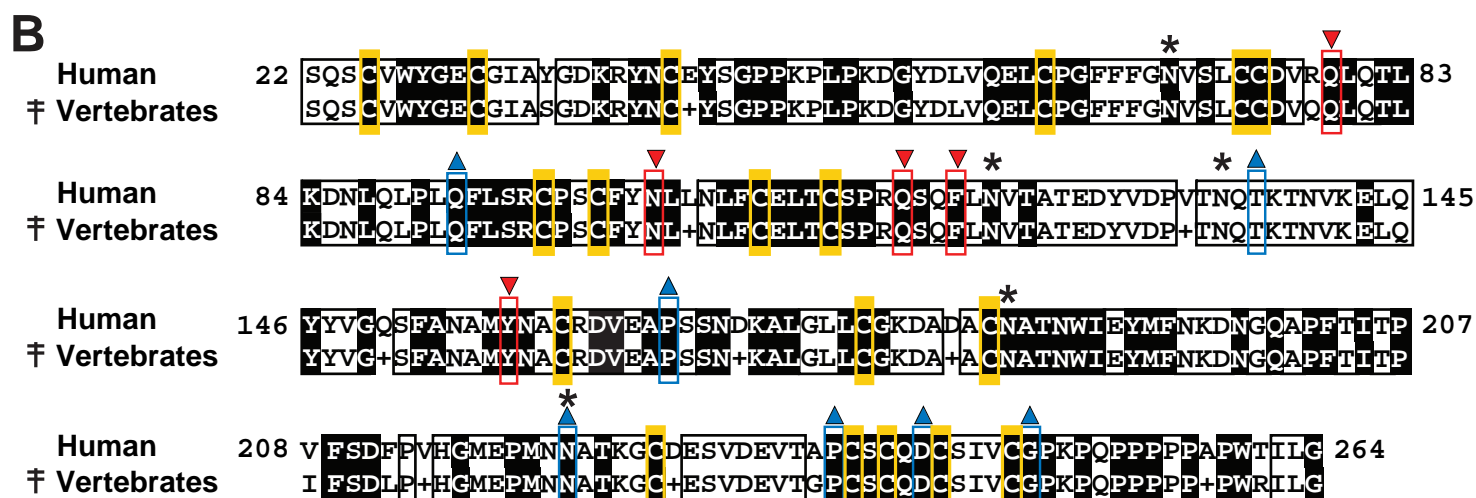
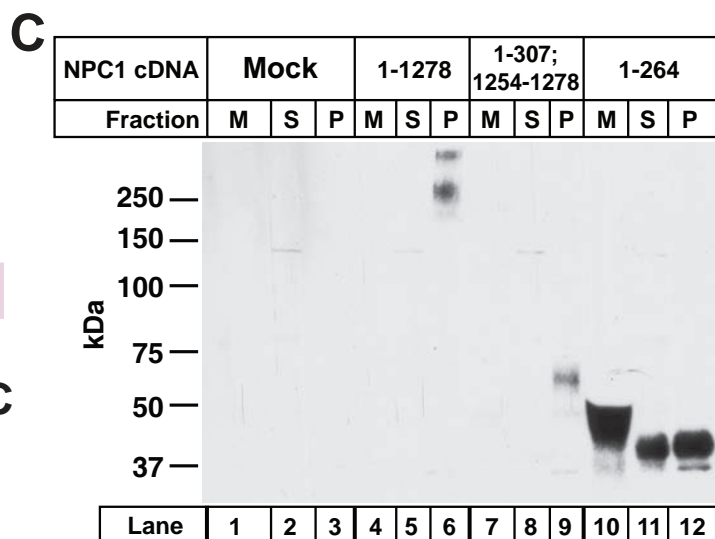
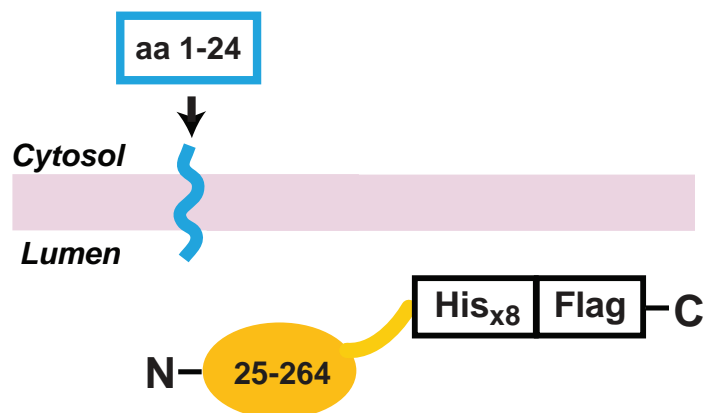
A Full-length NPC1(1-1278)



Internally Deleted NPC1 (1-307; 1254-1278)



C



‡ Consensus of 12 Species

Fig. 3

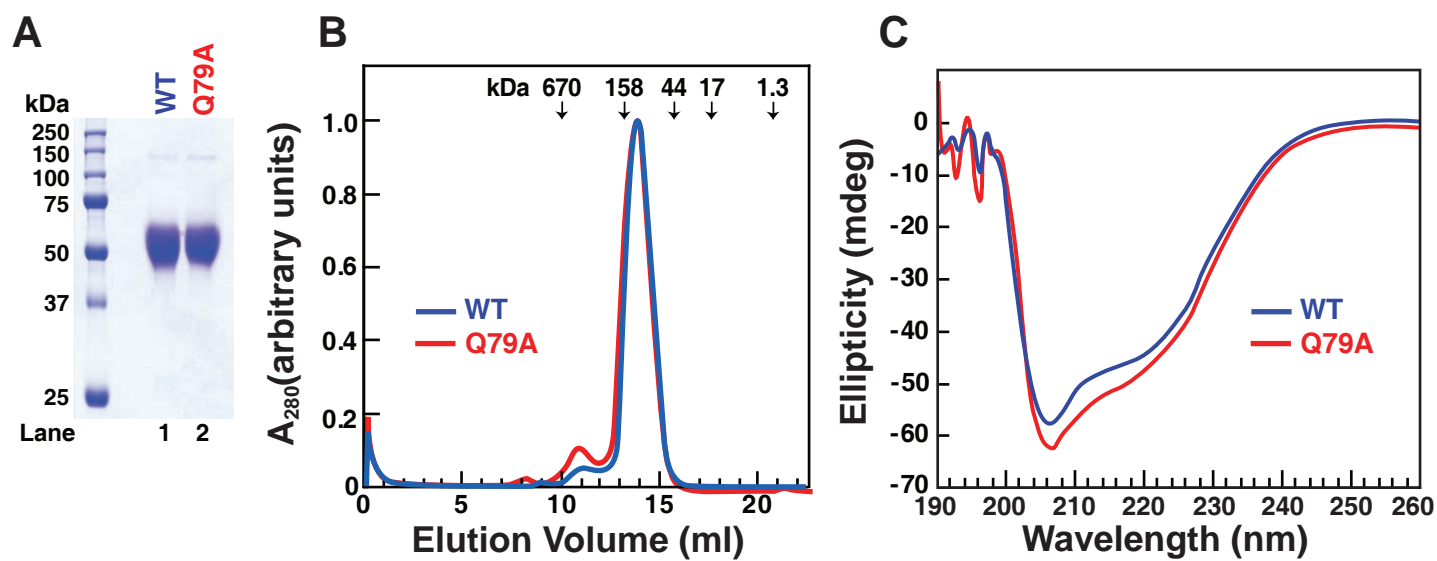


Fig. 4

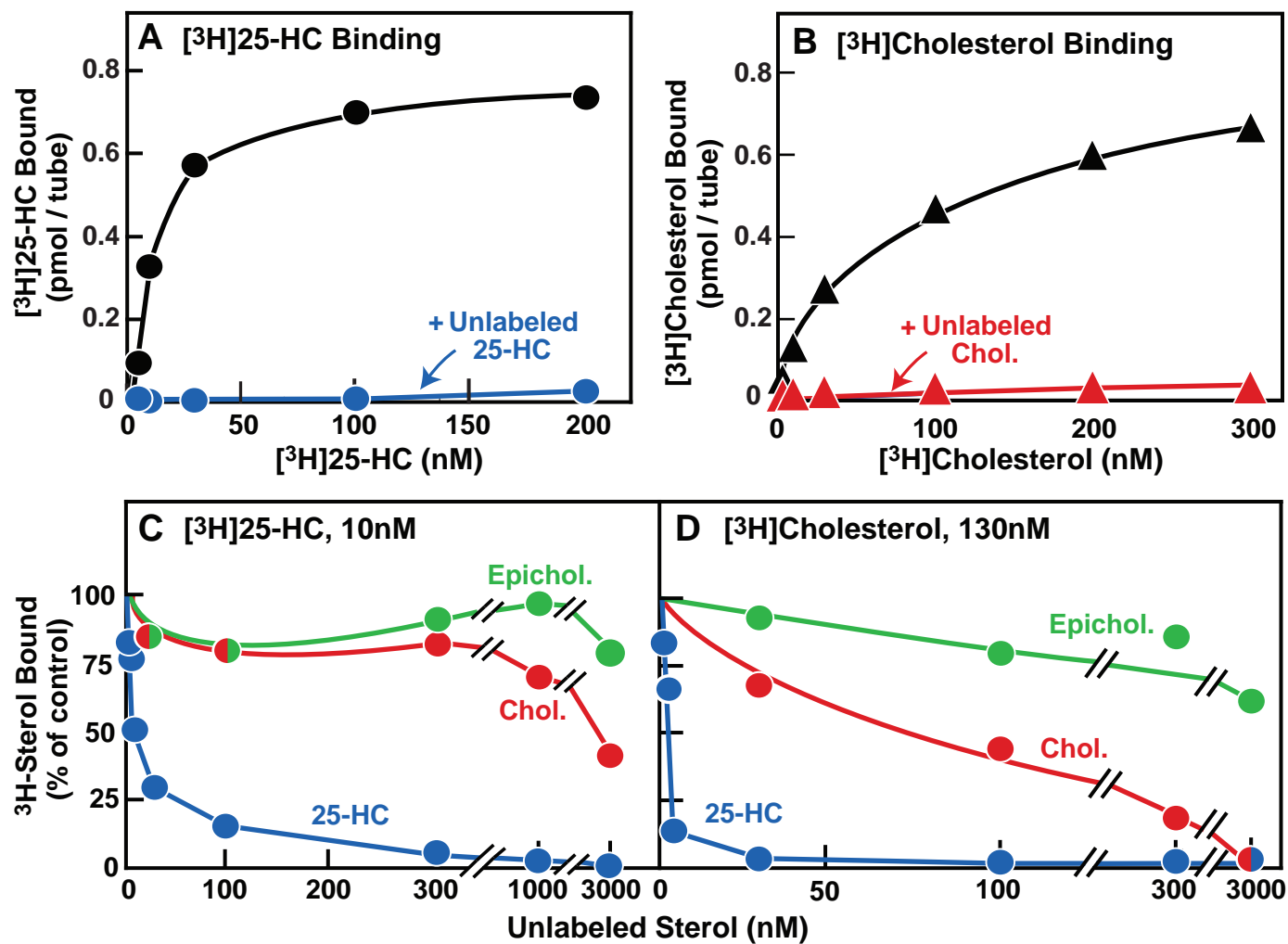


Fig. 5

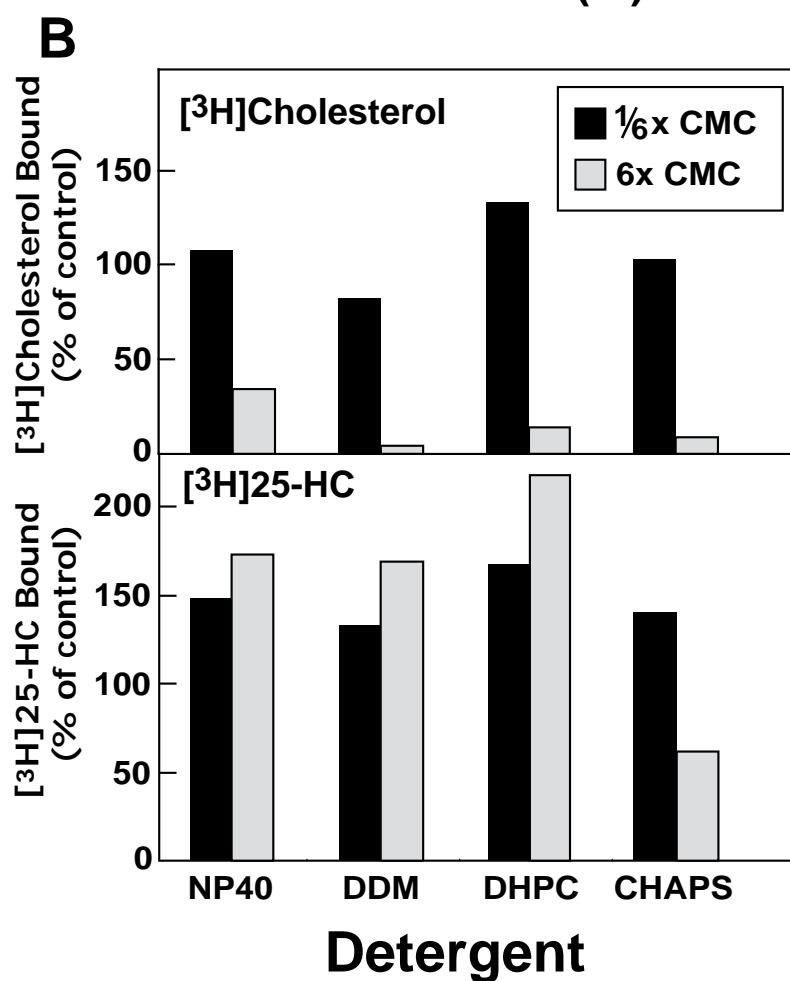
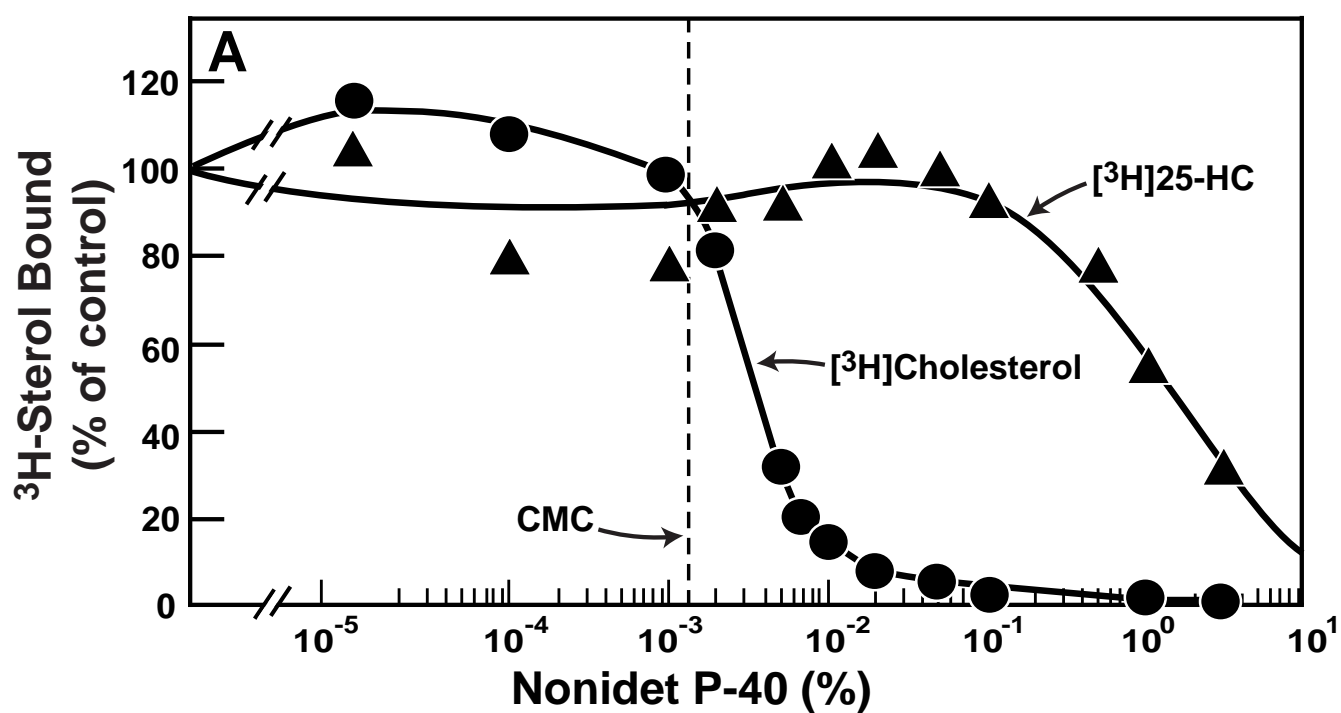


Fig. 6

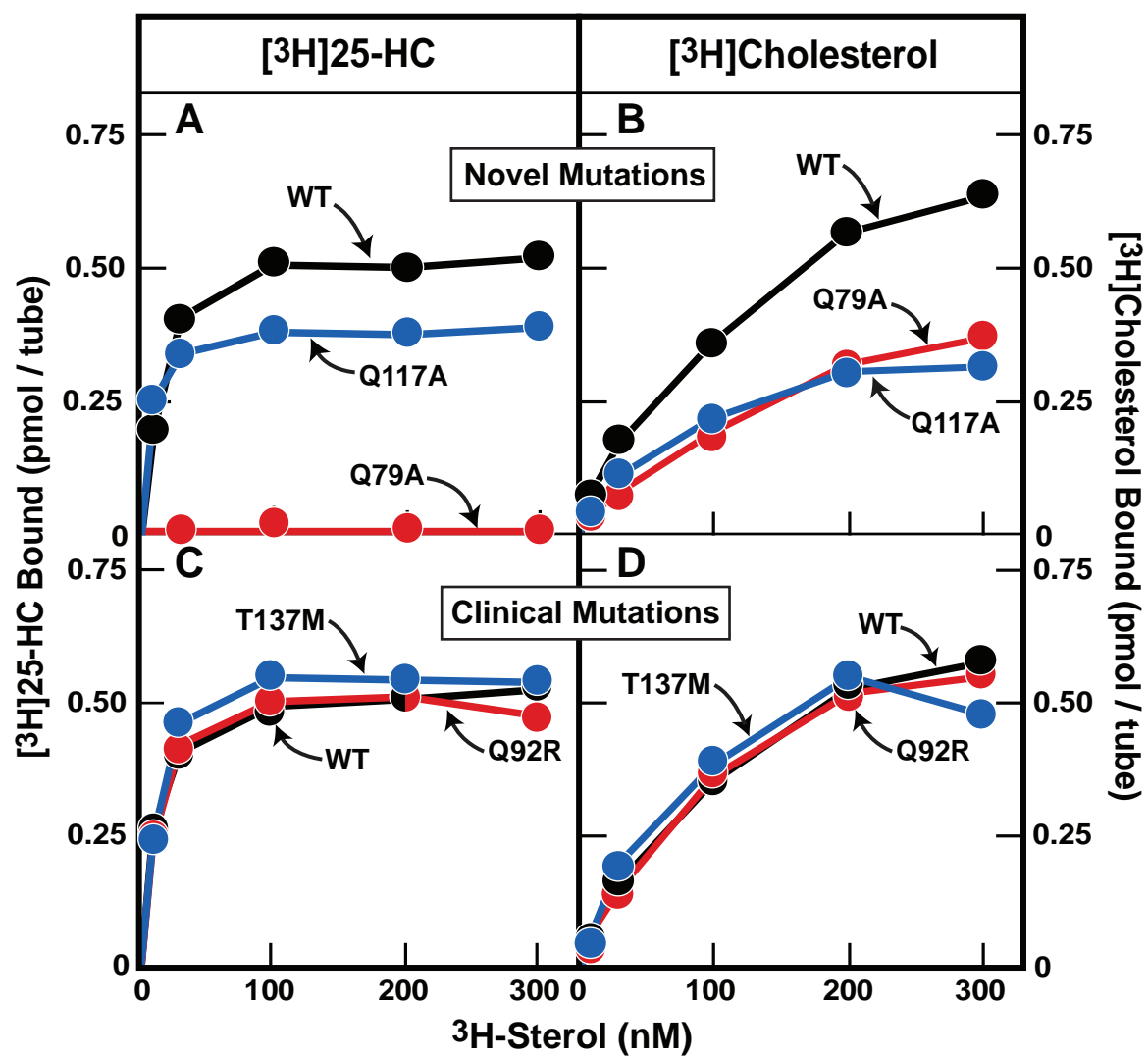


Fig. 7

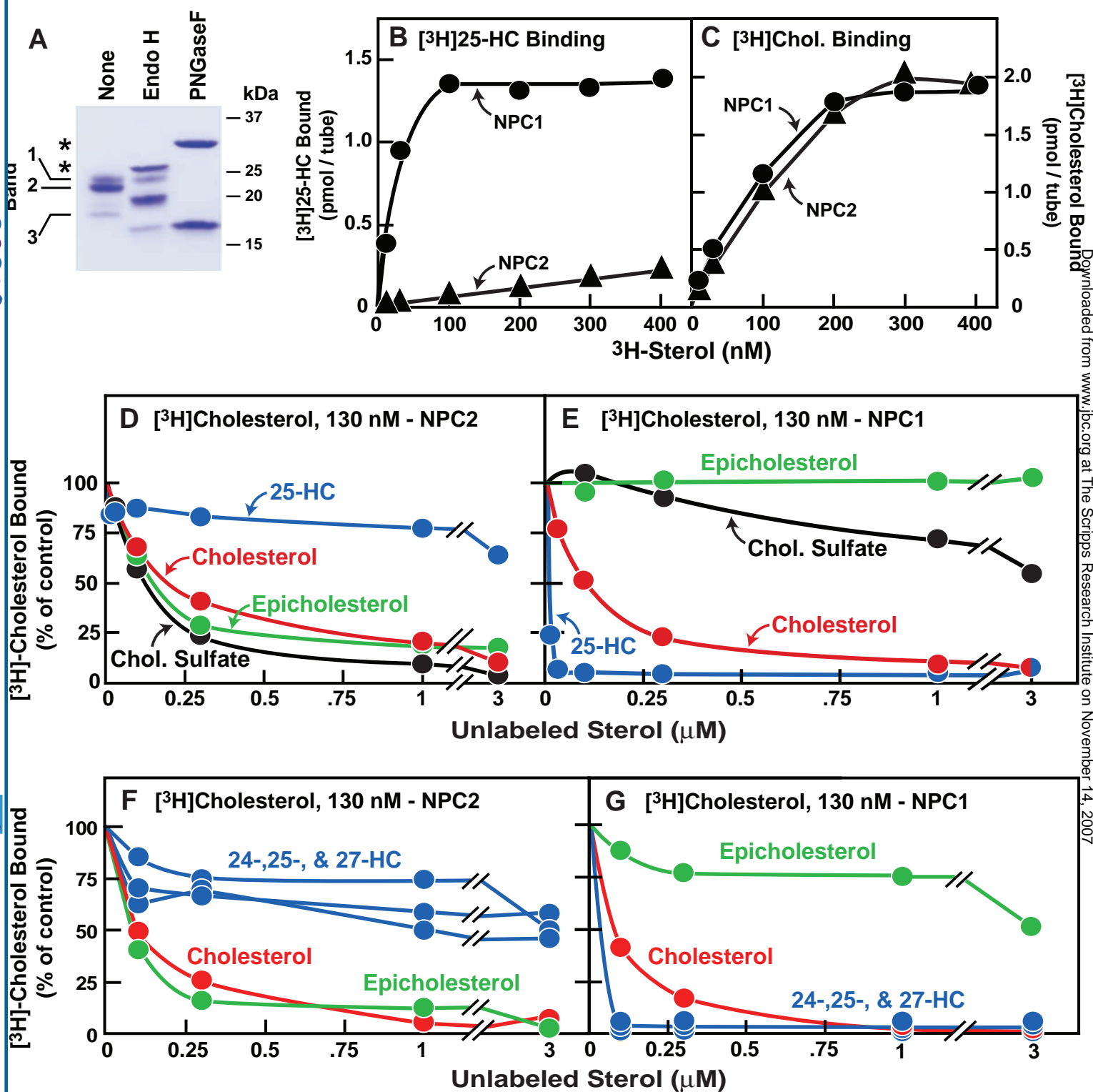


Fig. 8

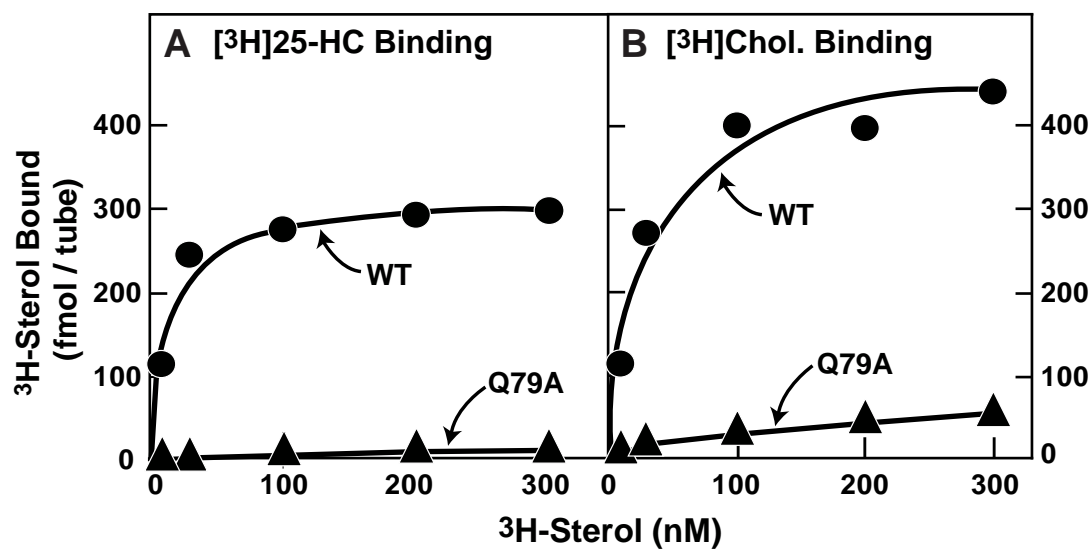


Fig. 9

